Cytometric features of cell nuclei of adenocarcinoma in situ and invasive adenocarcinoma of the cervix

Loyd A. West, MD,[a] Richard Swartz, MA,[b] Dennis Cox, PhD,[b] Iouri V. Boiko, MD,[d] Anais Malpica, MD,[a] Calum MacAulay, PhD,[e] and Michele Follen, MD, PhD[a,c]

Houston, Tex

OBJECTIVE: The goal of this study was to characterize adenocarcinoma in situ (ACIS) and invasive adenocarcinoma (AdCa) of the cervix by using image histometric measurements of nuclear morphometric features.
STUDY DESIGN: Archival pathology slides and tissue blocks from 37 patients with ACIS, 18 with invasive AdCa, and 13 with normal cervical epithelial and glandular histology were reviewed by two pathologists. The controls were matched for age and menstrual status and as closely as possible for the age of the slides; this limited the number of normal cases available. Morphometric, photometric, and textural measurements were made on 4-μm sections of tissue stained with a thionin-SO_2 Feulgen reaction. A mixed analysis of covariance model was used for analysis.
RESULTS: The Integrated Optical Density Index was found between the mean value for normal cells and that for ACIS and invasive AdCa ($P < .001$). Twenty-two other morphometric features were identified that exhibited differences in their means between at least two of the three tissue types.
CONCLUSION: In the cell populations studied, certain nuclear image features were found to correlate with histologic diagnosis. The features can be measured objectively and could be useful to pathologists in differentiating lesions, although a larger study should be evaluated to confirm these findings. Further, these features may be important as optical technologies are developed that make diagnoses in real time.
(Am J Obstet Gynecol 2002;187:1566-73.)

Key words: Image cytometry, adenocarcinoma, cervix uteri, carcinoma in situ

Adenocarcinoma in situ (ACIS) of the cervix was first described by Hepler et al in 1952[1] and further characterized by Friedell and McKay in 1953.[2] It is a relatively rare premalignant lesion, occurring in 1 per 25,000 Papanicolaou smears, but several studies suggest the incidence is increasing.[4,5] ACIS is the putative precursor of invasive adenocarcinoma (AdCa), which has a poorer prognosis than the more common squamous lesions of the cervix.[3,4,6,-9]

From the Departments of Gynecologic Oncology and Pathology, University of Texas M. D. Anderson Cancer Center,[a] the Department of Statistics, Rice University,[b] the Departments of Obstetrics, Gynecology, and Reproductive Sciences,[c] and the Department of Pathology,[d] University of Texas Health Science Center, and the British Columbia Cancer Agency, British Columbia Research Center.[e]
Supported by the National Cancer Institute grant No. PO1-CA 82710.
This article was written by LCDR Loyd A. West, MC, USNR, while a fellow at M. D. Anderson Cancer Center training in gynecologic oncology. The views expressed in this article are those of the author and do not reflect the official policy or position of the Department of the Navy, Department of Defense, or the US government.
Received for publication September 27, 2001; revised April 18, 2002; accepted June 21, 2002.
Reprint requests: Michele Follen, MD, PhD, Department of Gynecologic Oncology, University of Texas M. D. Anderson Cancer Center, 1515 Holcombe Blvd, Box 193, Houston, TX 77030.

0002-9378/2002 $35.00 + 0 ***6/1/127906***
doi:10.1067/mob.2002.127906

Well-defined cytologic and histologic diagnostic criteria were established relatively recently.[10-14] ACIS can resemble the nonspecific microscopic findings associated with it. ACIS can also resemble other lesions cytologically and histologically, including metaplasia, endometriosis, and reparative changes.[10] Therefore, traditional cytologic screening may not be sensitive for this lesion, and this may result in underdiagnosis of a potentially more serious clinical disease.[6,7] Also, distinguishing between preinvasive and invasive disease can be difficult.

Quantitative pathologic methods, including nuclear image analysis, have been developed to characterize the size, shape, DNA content, and patterns of chromatin distribution in cells, and to reduce the subjectivity of classic visual diagnostic interpretations. These methods provide objective, quantitative, and reproducible interpretation of the features seen in classic visual observations. The morphometric, photometric, and tissue features used by our group have been thoroughly described.[15] These quantitative pathologic techniques have also been exploited in commercially available image-analysis systems, some of which are designed for cervical cytologic diagnosis of squamous lesions. These systems typically measure, compute, and store optical properties of nuclei, including morphologic properties (size, shape, symmetry), DNA content (with stoichiometric staining techniques),

Table I. Authors studying quantitative features of normal endocervix, ACIS, and invasive AdCa

First author	*Year*	*Reference*	*Histology or cytology*	*Sample size*	*Principal finding*
Agorastos	1994	21	Histology	3 histologic cases of ACIS	DNA cytometry useful in distinguishing cancerous from normal tissue
Biesterfeld	2001	22	Cytology	Pap smears: 65, normal; 18, inflammation; 22 invasive AdCa	DNA single-cell cytometry was higher in deviant groups
Boon	1981	6	Histology	5 histologic cases of ACIS	Significant differences between benign epithelium and ACIS were found in nuclear perimeter, cell horizontal axis, nuclear vertical axis, ratio cellular axes, and nuclear/cytoplasmic size ratio
Gloor	1982	23	Histology	14 histologic cases of ACIS	Distinguished 2 types of ACIS by histology
van-Aspert–van-Erp	1997	24	Cytology	50 Pap smears from 48 patients with ACIS	Five features highly related to the correct diagnosis: cell arrangement, cytoplasmic vacuolation, variable nuclear size and shape, chromatin characteristics, and nucleolar characteristics
Van Roon	1983	25	Histology	20 patients with normal cervix, 11 histologic cases of ACIS	Changes in glandular and cellular architecture helpful in distinguishing disease

Pap, Papanicolaou.

and texture features based on the digital image of the cell.[15] Such nuclear features may be related to the ploidy of the cell and the degree of abnormality, allowing a quantification of the degree of abnormality that can be correlated with other biomarkers to evaluate ploidy.[16,17]

Certain nuclear features have proved useful in other tissue models to discriminate between normal, premalignant, and malignant cell types. These methods may also have the potential to detect premalignant lesions before DNA changes can be detected by classic visual techniques.[18] These features have also been used successfully to monitor regression/progression in chemoprevention studies for premalignant conditions.[19,20] Characterization of certain image features of the normal cervix, ACIS, and invasive AdCa may allow discrimination between these lesions with automated methods, resulting in improved diagnostic capabilities.

These lesions are rare; to date, six other groups have conducted studies of each.[6,21-25] These studies and their findings are listed in Table I. Our group is investigating noninvasive optical diagnostic tools for cervical pathology. Characterization of nuclear features with image analysis techniques may be useful in developing optical diagnostic methods for these glandular cervical lesions.

Material and methods

Patient case selection. A retrospective computerized search by pathologic diagnosis of the Department of Pathology records at the M. D. Anderson Cancer Center was performed. Archival tissue blocks and pathology slides stained with hematoxylin and eosin (H&E) were reviewed and mapped by two pathologists having gynecologic specialization (A. M., I. V. B.). The diagnosis of ACIS and invasive AdCa was confirmed by established criteria.[11-14] Cases containing mixed lesions or insufficient tissue for subsequent preparation and analysis were excluded. Thirty-seven patients with ACIS, 18 with adenocarcinoma, and 13 with normal epithelial and glandular histology were included in the final analysis. The clinical performance of this group of patients is described elsewhere.[26] The controls were matched for age and menstrual status and as closely as possible for the age of the slides; this limited the number of normal cases available. None of the controls had significant inflammation in the tissue. Few hysterectomies are performed at M. D. Anderson for benign conditions, which also restricted the number of controls available for this study. In addition, our neighboring institutions fix tissue by using different fixation protocols, and we thought it was important to have uniform fixation for all samples. We analyzed histologic notes and data from 37 patients with ACIS, 18 with invasive AdCa, and 13 with normal cervical histologic studies. The patient and tissue characteristics and the number of cells measured are tabulated in Table II.

Specimen preparation. All specimens were prepared by using similar preparation techniques. Sections 4 μm thick were cut from the formalin-fixed, paraffin-embedded archival surgical specimens and stained with a thionin-Feulgen reaction method as previously described by our group[19] and with respect to previously noted limitations

Table II. Statistical parameters of age and tissue characteristics for the study population

	Normal endocervix	*Adenocarcinoma in situ*	*Invasive adenocarcinoma*
No. of patients	13	37	18
Mean age (y)	46.1	37.9	41.3
SD (y)	9.4	9.2	15.3
Age range (y)	23-68	25-62	26–78
No. of histologic sections	13	37	18
No. of epithelial cells measured per histologic section (mean ± SD)	134 ± 35	130 ± 43	200 ± 64
No. of lymphocyte cells measured per histologic section (for normalization) (mean ± SD)	107 ± 54	111 ± 33	94 ± 48

by other prominent investigators.[27-31] One histotechnologist cut all the sections on the same system, and in an additional set of clinical material not included in this study, the variability of the sectioning of this histotechnologist and microtome was found to produce sections which varied less than ±0.5 μm over multiple cuts and multiple samples (data unpublished). The slides were then reviewed and compared with the original H&E slides to confirm the diagnosis and that there was sufficient tissue for analysis. The pathologist mapped the areas on each slide containing the tissue of interest for image analysis.

Image analysis and cell selection. A CytoSavant computer-assisted image analysis system (Oncometrics Imaging Co, Vancouver, Canada) was used for image cytometric measurement of nuclear features. Lymphocytes were used as an internal standard to normalize each slide and to control for staining variation. Measurement of the staining-intensity-normalized Integrated Optical Density in the sections (IODs-Index) was calculated based on the ratio of the integrated optical density of each nucleus to that of internal lymphocyte reference cells.[20] Data were collected from a total of 75 patients, with one histologic section per patient, but data from two specimens had to be discarded because normalization could not be carried out. Five other slides had out-of-focus images and were also discarded. For each of the remaining 68 tissue sections, nuclear images of lymphocytes and epithelial nuclei were collected from areas mapped by the pathologist and the investigators (L. W., I. V. B.). Only nonoverlapping nuclei with easily discernible borders were used for analysis.[29,30]

Statistical analysis and techniques. All statistical analyses were performed with SAS version 8.01 (Cary, NC). The mean age across the three diagnostic groups was examined with a one-way analysis of variance (ANOVA). The nuclear features were examined using a mixed-effects analysis of covariance model. To meet the assumption that the data are normally distributed, we first transformed the data by using a Box-Cox procedure, which estimates the power transform necessary to achieve normalcy.[32] The given mixed model was then fit to the transformed data by using the restricted maximum-likelihood method implemented in the MIXED procedure in SAS.[36,37] Because tissue characteristics change with age and the subjects in this study were not matched on that variable, age was included as a covariate to adjust for any confounding effects it might have.

The mixed model with the age covariate is specified as follows[32,38]:

$$y_{ijk} = \mu + \alpha x_{ij} + \beta_i + \gamma_j + \varepsilon_{ijk},$$

where x_{ij} is the age of patient j with cell type i, y_{ijk} is the measured feature value for cell k of type i from patient j, μ is a constant representing the overall mean of the scores, α is the regression coefficient for the age effect, and β_i represents the contribution of cell type i to the scores subject to the constraint $\sum_i \beta_i = 0$. The term $\sum_i \gamma_j$ represents a random effect due to patient j. These effects are assumed to be independently distributed, normal random variables with mean 0 and variance τ^2. The usual error term for a regression model, ε_{ijk}, is assumed to be independently distributed normal random variables with mean 0 and variance σ^2.

The simultaneous test for significance of the cell type effects ($\beta_{AdCa} = \beta_{ACIS} = \beta_{normal} = 0$) was performed separately for the IODs-Index measurement because there was a biologic reason that this variable should be different. For the other 58 features, to keep the family-wise error rate at the usual .05 α level, we adjusted the *P* values for multiple comparisons using both the sharpened step-down Holm procedure and the sharpened step-up Hochberg procedure. Both methods produced the same subset of features, maintaining significant *P* values after adjustment. This same technique was applied when testing the significance of the age covariate, and again both methods agreed. The step-down method orders the *P* values from smallest to largest, and once a *P* value is found to be large enough that it is not rejected according to some criteria that are a function of the family-wise error rate, all larger *P* values are retained. The step-up method orders all *P* values from largest to smallest, and once a *P* value is found to be small according to a criterion that is again a function of the family-wise error rate, all smaller *P* values are rejected. *Sharpened* refers to the fact that these

Table III. Significant group differences of morphometric features*

	P values (Bonferonni adjusted)		
Feature	*Norm vs ACIS*	*Norm vs invasive AdCa*	*ACIS vs invasive AdCa*
High-average distance	**<.001**†	**<.001**†	**<.038**‡
Density dark spot	**<.001**†	**<.001**†	**<.013**‡
Cluster prominence	**<.001**†	**<.001**†	**<.001**†
IODs-Index§	<.001†	<.001†	.507
Medium-density objects	<.001†	<.001†	.338
Density light spot	.018‡	<.001†	.163
Medium center of mass	<.001†	.044‡	.080
Compactness	<.001†	>.999	<.001†
Eccentricity	<.001†	>.999	<.001†
Inertia shape	<.001†	>.999	<.001†
Sphericity	.002†	.762	<.001†
Medium/high-average distance	<.001†	>.999	<.001†
Low-average distance	<.001†	>.999	.002†
Low vs medium DNA	.002†	>.999	.003‡
Low DNA amount	< .001†	>.999	.010‡
Low DNA compactness	.002†	>.999	.003†
Variance of radius	<.001†	.751	.011‡
Low vs high DNA	.013‡	>.999	.016‡
Low-density objects	.016‡	>.999	.006‡
Short run length (135 degrees)	.543	.004†	.039‡
OD kurtosis	.198	<.001†	.011†
Entropy	.111	< .001†	.019‡
Energy	.380	.003†	.063

Bold *P* values indicate features with significant differences among all three cell types.

*These features were found to be significant after adjusting for multiple comparisons using both the sharpened step-up Hochberg and the sharpened step-down Holm family-wise procedures. Error rate for the pairwise comparison is controlled using the Bonferroni adjustment.

†Significant at the .01 level.

‡Significant at the .05 level.

§IODs-Index, examined independently and was not included when correcting family-wise error rates for the other features.

particular procedures use an estimate of the number of *P* values that would arise from true null hypotheses to improve the ordinary Holm or Hochberg adjustment procedures.[39] Because the simultaneous test for significance gives no insight into the particular groups that differ, we examined the pairwise differences for each feature that had a significant cell-type effect. The pairwise comparisons within each significant feature were adjusted by using the Bonferonni method of adjusting for multiple comparisons.

We restricted our analysis to 59 features that were determined to be independent of staining technique. Because of logistic constraints, we did not have the capability to simultaneously stain all study slides in a single batch with the Feulgen reaction. Therefore, we eliminated features that would be affected by differences in stain intensity, eliminating any confounding effect staining intensity might have on detecting differences among the three cell types. Because of these constraints, the statistical analysis performed was appropriate for the data set. Larger numbers of well-classified specimens, stained in random batches, and matched for age of control slides will be collected. This will allow the larger data sets that would be required for discriminant analysis and classification algorithms to be generated.[33,34,35] This is anticipated future work.

Results

Nuclear features of cervical histologic sections, including normal tissue, ACIS, and invasive AdCa, have been evaluated and quantified with automated imaging techniques, and some of these features were found to correlate with tissue diagnoses. A list of the significant features, and the groups found to be different, can be found in Table III.

It is known that the characteristics of human tissue change with age; however, we were unsure whether the characteristics of the individual cell nuclei would vary with age in this study. Therefore, we explored possible age effects. Although age varied across the three groups (Table II), the differences were not statistically significant ($P = .059$). However, one can notice that the variances within each group differ, and in the ANOVA model, this results in a loss of power to detect a significant difference. Also, our *P* value, although not significant at the .05 level, was approaching significance. Therefore, to be conservative, we still included age in the mixed models to adjust for any possible effect.

Table IV. Image feature definitions

Feature	*Order**	*Biologic implication*
High-average distance	Norm < AdCa < ACIS	High-chromatin density pixels of normal cells are more evenly distributed in the nucleus, with ACIS being the least evenly distributed
Density dark spot	Norm < ACIS < AdCa	As a lesion progresses toward cancer, the number of pixels having a local maximum concentration of chromatin increases
Cluster prominence	Norm < ACIS < AdCa	As a lesion progresses from normal to ACIS to AdCa, nuclei have more defined and distinct clumps of chromatin in the nucleus
IODs-Index	Norm < ACIS, AdCa	Precancerous/malignant cell nuclei have more DNA material on average
Medium-density objects	Norm < ACIS, AdCa	More medium-chromatin density clumps are found in the ACIS and AdCa nuclei
Density light spot	Norm < ACIS, AdCa	More pixels with local minimum concentration of chromatin in the cancer cell nuclei (ACIS, AdCa)
Medium center of mass	Norm < AdCa, ACIS	Center of mass of the medium-chromatin components is farther from the geometric center for the ACIS nuclei than for the normal nuclei
Compactness	AdCa, Norm < ACIS	ACIS nucleus boundary is irregular compared with the more circular normal and AdCa nuclei
Eccentricity	Norm, AdCa < ACIS	ACIS cell nuclei are more irregular (less circular)
Inertia shape	AdCa, Norm < ACIS	Mass is distributed less uniformly for ACIS nuclei
Sphericity	ACIS < Norm, AdCa	ACIS nuclei are less circular
Medium/high-average distance	Norm, AdCa < ACIS	The average distance from the geometric center (among the high- and medium-chromatin pixels) is higher in the ACIS nuclei than for the normal nuclei
Low-average distance	ACIS < AdCa, Norm	The low-chromatin components of the ACIS nuclei are located closer to the geometric center than are those of the AdCa and normal nuclei
Low vs medium DNA	Norm, AdCa < ACIS	Measures the ratio of MOD[c] of the medium-chromatin condensation relative to the low-chromatin condensation. The ACIS nuclei on average have higher ratios
Low DNA amount	ACIS < AdCa, Norm	There is more DNA in the disperse clumps of low DNA chromatin (relative to the total DNA) for the AdCa and normal nuclei than the ACIS nuclei
Low DNA compactness	ACIS < AdCa < Norm	Clumps of low-chromatin concentration within the nuclei are more irregularly shaped for AdCa and normal cell nuclei than for ACIS cell nuclei
Variance of radius	Norm, AdCa < ACIS	The boundary of the ACIS nucleus is more irregular than those of the AdCa and normal nuclei
Low vs high DNA	Norm, AdCa < ACIS	Ratio of MOD of the high-chromatin condensation relative to that of the low-chromatin condensation
Low-density objects	ACIS < AdCa, Norm	Fewer low-chromatin density clumps are found in the ACIS nuclei
Short run length 135	AdCa < ACIS, Norm	Not many pixels of the same gray scale level are contiguous, suggesting clumping The run length texture features are not invariant with respect to the orientation of the cell within the image field. The fact that this feature is significant suggests that all short run length features can contain information
OD kurtosis	Norm, ACIS < AdCa	The distribution of the OD seems to have fatter tails and be more peaked as the lesion progresses in malignancy
Entropy	AdCa < ACIS, Norm	Measure of disorder of the distribution of chromatin in the nucleus. The AdCa nuclei have more organized domains of similar chromatin structures
Energy	Norm < AdCa†	Measure of nonuniformity of DNA distribution within the nucleus—progressing from normal to cancerous, the nuclei are more nonuniform

Norm, Normal; *MOD,* mean optical density; *OD,* optical density.

*Comma denotes an ordering without a significant difference between the groups; < indicates an ordering with a significant difference.

†ACIS is omitted from this column because it fell between the 2 groups but was not significantly different from either.

A mixed-model analysis of Box-Cox transformed IODs-Index and other morphometric nuclear features revealed that the IODs-Index and 22 other features exhibit significant differences between normal cells and either ACIS or invasive AdCa or both. A mixed model was used because the γ_j terms introduce an added flexibility to the model that allows us to account for the intrapatient variability incurred by sampling several cells from the same patient. Implicit in these assumptions is that the observed scores are distributed according to a normal distribution with a given mean and variance structure. The data, however, were not found to be normal, and in an attempt to achieve normalcy, the Box-Cox transformation was applied to each feature before analysis with the mixed

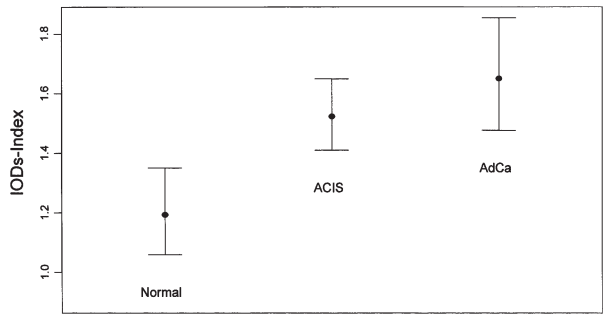

Fig 1. IODs-Index versus cervix tissue type. IODs-Index, a measure of DNA content, provides a basis for distinguishing normal from ACIS or invasive AdCa cells. Cervix tissue type, 95% CI (Bonferonni adjusted).

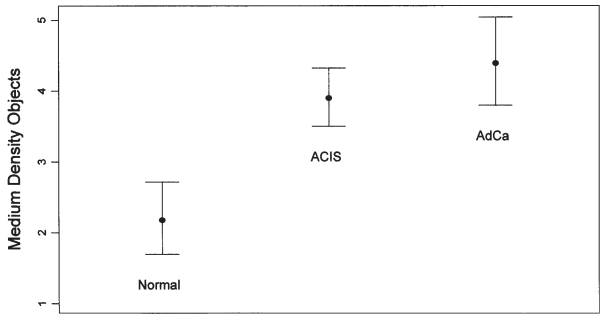

Fig 2. Medium-density objects versus cervix tissue type. Medium-density objects, a measure of medium-density chromatin clumping in the nucleus, is less for the normal cells than for ACIS and invasive AdCa. Cervix tissue type, 95% CI (Bonferonni adjusted).

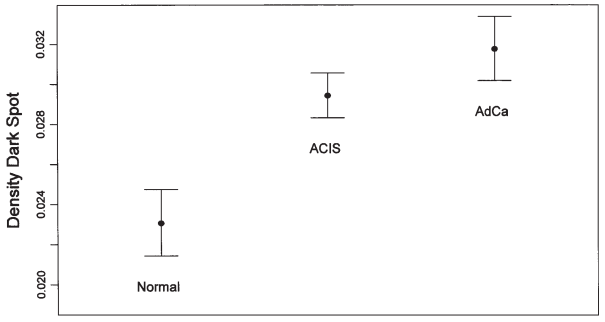

Fig 3. Density dark spot versus cervix tissue type. Density dark spot, a measure of local concentration of chromatin, shows a clear distinction between normal cells and ACIS or invasive AdCa cells. Cervix tissue type, 95% CI (Bonferonni adjusted).

model. With several features, the transformations were not fully successful in achieving normality. Under the mixed model and other ANCOVA approaches, this typically results in a reduction in power for the technique, while the alpha level is relatively unaffected.[40]

The mixed-model analysis of the Box-Cox transformed IODs-Index revealed significant differences between the

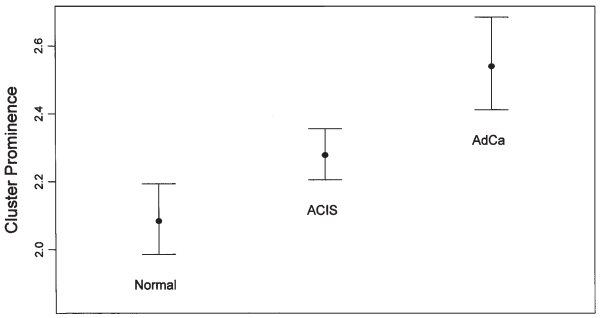

Fig 4. Cluster prominence versus cervix tissue type. Cluster prominence, a measure of chromatin clumping, provides distinction among all 3 cell types. Cervix tissue type, 95% CI (Bonferonni adjusted).

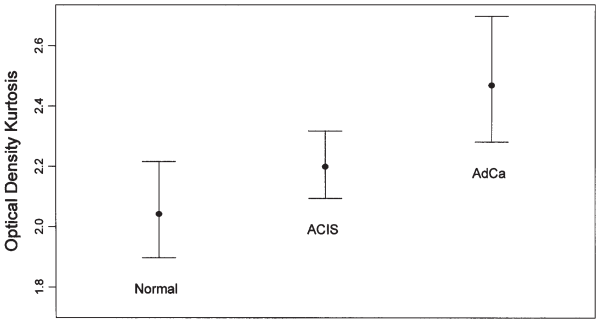

Fig 5. OD kurtosis versus cervix tissue type. OD kurtosis identifies the invasive AdCa cells, reflecting their distinctly different optical density distributions. Cervix tissue type, 95% CI (Bonferonni adjusted).

normal cells and the ACIS and invasive AdCa cell types, indicating a greater amount of DNA in the last two (Table III, Fig 1). Although not reaching statistical significance, the IODs-Index value was higher in invasive AdCa than in the preinvasive ACIS. This higher IODs-Index value, indicative of more DNA material in the cancerous cells, has been seen in other studies.[41]

Of the 58 other stain-independent morphology and texture features, 22 showed significant differences among the three histologic tissue diagnoses. The features in Table III have been ordered so that the three features that have statistically significant differences among all three cell types are placed at the top, and the following features are ordered according to the significance of the differences among the three cell types. The first feature, high-average distance, measures the distribution of high-chromatin density pixels in cell nuclei. The next two features, density dark spot and cluster prominence, measure the concentration and appearance of chromatin in the nuclei, respectively. IODs-Index is a measure of nuclear DNA content. The subsequent 19 features have statistically significant differences between two of the three cell types. The next three features, medium-density objects,

density light spot, and medium center of mass, measure properties related to the density and distribution of chromatin in the nucleus. Compactness and eccentricity relate to the irregular shape of the ACIS nuclear boundary, compared with the more circular shape of the normal and invasive AdCa nuclei. The next feature, inertia shape, refers to the distribution of mass within the nucleus. Sphericity also refers to the shape of the nuclear boundary. The next two features, medium/high-average distance and low-average distance, measure the location of chromatin in the nucleus. Low versus medium DNA and low DNA amount are measures of chromatin in the nucleus. (Low DNA compactness relates to the irregular shape of clumps of low-chromatin concentration in invasive AdCa and normal cell nuclei compared with ACIS nuclei.) Variance of radius refers to the irregular boundary of ACIS nuclei. The next feature, low versus high DNA, is a measure of the high-chromatin condensation relative to that of the low-chromatin condensation. A measure of low-density objects shows that ACIS nuclei have fewer low-chromatin density clumps. The next feature, short run length 135, shows clumping in pixels of invasive AdCa nuclei. The next two features, optical density (OD) kurtosis and entropy, distinguish, by the clumping of chromatin, invasive AdCa from the normal and ACIS cells. The last feature, energy, shows a statistically significant difference only between normal and invasive AdCa cells; it measures the nonuniformity of DNA distribution within the nucleus, which progresses as the cells become cancerous. Table IV lists the features, relative values of the features for the three tissue types, and their biologic implications.

The figures illustrate the visually compelling differences in the quantitative features. Fig 1, the plot of the IODs-Indexes, demonstrates the statistically significant separation of normal tissue from ACIS and invasive AdCa. Fig 2 demonstrates the statistically significant difference in medium-density objects between normal, ACIS, and invasive AdCa cell types. Fig 3, a plot of density dark spot, shows how the local maximum concentration of chromatin increases as cells progress from normal to ACIS to invasive AdCa. Cluster prominence (Fig 4), a measure of the distinction of chromatin clumps in the nuclei, shows significant differences between all three cell types. Fig 5, a plot of OD kurtosis, distinguishes invasive AdCa from the normal and ACIS cells. All the plots (Figs 1-5) are shown with Bonferonni-adjusted 95% CIs.

Comment

This study evaluated nuclear features from a well-classified selection of ACIS and invasive AdCa cases. The ACIS cases were collected as part of a review paper concerning the clinical performance of ACIS of patients at the M. D. Anderson Cancer Center. At the time of this published review, all the available ACIS cases were included; those that were not included in this study did not have additional material for quantitative staining available. The normal endocervix cases were selected randomly from our database and matched for age and menstrual status. These findings should be confirmed in a larger dataset of equivalently well-selected and well-classified independent samples. We have identified several features that correlate with histologic diagnosis, some of which are statistically distinct among all three tissue types. We specifically selected features that are independent of staining technique, allowing comparison of tissues obtained or stained at different times.

The image features we have analyzed could be used to develop and validate future automated diagnostic algorithms. This may allow development of automatic screening and diagnostic techniques such as those developed for screening Papanicolaou smears. Further analysis is needed to develop diagnostic algorithms and determine performance characteristics of this technology with respect to the detection and evaluation of these lesions. We will need to apply similar techniques to cytologic material to determine whether these methods are valid for commonly obtained cervical screening specimens. We will also need to evaluate the performance of this technology in the presence of adenomatous-squamous lesions.

We are currently investigating noninvasive optical diagnostic tools for cervical pathology. Characterization of nuclear features with image analysis techniques may be useful in developing optical diagnostic methods for glandular cervical lesions. Identification of image features relevant to ACIS and invasive AdCa may guide future development of diagnostic procedures using techniques such as in vivo confocal microscopy and reflectance spectroscopy. Both of these technologies examine chromatin quantitatively. This may lead to more definitive diagnoses of these lesions in real time.

REFERENCES

1. Hepler T, Dockerty M, Randall L. Primary adenocarcinoma of the cervix. Am J Obstet Gynecol 1952;63:800-8.
2. Friedell G, McKay D. Adenocarcinoma in situ of the endocervix. Cancer 1953;6:887-97.
3. Weisbrot I, Stabinski C, Davis A. Adenocarcinoma in situ of the uterine cervix. Cancer 1972;29:1179-87.
4. Christopherson WM, Nelson N, Gray LA. Noninvasive precursor lesions of adenocarcinoma and mixed adenosquamous carcinoma of the cervix uteri. Cancer 1979;44:975-83.
5. Peters RK, Chao A, Mack TM, Thomas D, Berstein L, Henderson BE. Increased frequency of adenocarcinoma of the uterine cervix in young women in Los Angeles County. J Natl Cancer Inst 1986;76:423-8.
6. Boon ME, Baak JPA, Kurver PJH, Overdiep SH, Verdonk GW. Adenocarcinoma in situ of the cervix: an underdiagnosed lesion. Cancer 1981;48:768-73.
7. Lee KR, Minter LJ, Granter S. Papanicolaou smear sensitivity for adenocarcinoma in situ of cervix: a study of 34 cases. Anal Cell Pathol 1997;107:30-5.
8. Drescher CW, Hopkins MP, Roberts JA. Comparison of the pattern of metastatic spread of squamous cell cancer and adenocarcinoma of the uterine cervix. Gynecol Oncol 1989;33:340-3.

9. Eifel PJ, Burke TW, Morris M, Smith TL. Adenocarcinoma as an independent risk factor for disease recurrence in patients with stage IB cervical carcinoma. Gynecol Oncol 1995;59:38-44.
10. Im DD, Duska LR, Rosenshein ND. Adequacy of conization margins in adenocarcinoma in situ of the cervix as a predictor of residual disease. Gynecol Oncol 1995;59:179-82.
11. Krumins I, Young Q, Pacey F, Bousfield L, Mulhearn L. The cytologic diagnosis of adenocarcinoma in situ of the cervix uteri. Acta Cytol 1977;21:320-9.
12. Bousfield L, Pacey F, Young Q, Krumins I, Osborn R. The expanded cytologic criteria for the diagnosis of adenocarcinoma in situ of the cervix and related lesions. Acta Cytol 1980;24: 283-96.
13. Ayer B, Pacey F, Greenberg M, Bousfield L. The cytologic diagnosis of adenocarcinoma in situ of the cervix uteri and related lesions. Acta Cytol 1987;31:397-411.
14. Ballo MS, Siverberg SG, Sidaway MK. Cytologic features of well-differentiated villoglandular adenocarcinoma of the cervix. Acta Cytol 1996;40:536-40.
15. Doudkine A, MacAulay C, Poulin N, Palcic B. Nuclear texture measurements in image cytometry. Pathologica 1995;87:286-99.
16. Partington CK, Sincouk AM, Steele SJ. Quantitative determination of acid-labile DNA in cervical intraepithelial neoplasia. Cancer 1991;67:3104-9.
17. Mitchell MF, Hittelman WN, Hong WK, Lotan R, Schottenfeld D. The natural history of cervical intraepithelial neoplasia: an argument for intermediate endpoint biomarkers. Cancer Epidemiol Biomarkers Prev 1994;3:619-26.
18. MacAulay C, Lam S, Payne PW, LeRiche JC, Palcic B. Malignancy-associated changes in bronchial epithelial cells in biopsy specimens. Anal Quant Cytol Histol 1995;17:55-61.
19. Boiko IV, Mitchell MF, Pandey DK, White RA, Hu W, Malpica A, et al. DNA image cytometric measurement as a surrogate endpoint biomarker in a phase I trial of α-difluoromethylornithine for cervical intraepithelial neoplasia. Cancer Epidemiol Biomarkers Prev 1997;6:849-55.
20. Poulin N, Boiko I, MacAulay C, Boone C, Nishioka K, Hittelman W, et al. Nuclear morphometry as an intermediate endpoint biomarker in chemoprevention of cervical carcinoma using α-difluoromethylornithine. Cytometry 1999;38:214-23.
21. Agorastos T, Andromache V, Papaloucas A. Minimal deviation adenocarcinoma of the cervix: A hypodiploid tumor? Int J Gynecol Pathol 1994;13:211-9.
22. Biesterfeld S, Reus K, Bayer-Pietsch E, Mihalcea AM, Böcking A. DNA image cytometry in the differential diagnosis of endocervical adenocarcinoma. Cancer (Cancer Cytopathol) 2001;93: 160-4.
23. Gloor E, Ruaicka J. Morphology of adenocarcinoma in situ of the uterine cervix: a study of 14 cases. Cancer 1982;49:294-302.
24. van-Aspert–van-Erp AJM, van't Hof–Grootenboer BE, Brugal G, Vooijs GP. Identifying cytologic characteristics and grading endocervical columnar cell abnormalities: a study aided by high-definition television. Acta Cytol 1997;41:1659-70.
25. Van Roon E, Boon ME, Kurver PJH, Baak JPA. The association between precancerous-columnar and squamous lesions of the cervix: a morphometric study. Histopathology 1983;7:887-96.
26. Wolf JK, Levenback C, Malpica A, Morris M, Burke R, Mitchell MF. Adenocarcinoma in situ of the cervix: significance of cone biopsy margins. Obstet Gynecol 1996;88:82-6.
27. Baak JPA, Noteboom E, Koevoets JJM. The influence of fixative and other variations in tissue processing on nuclear morphometric features. Anal Quant Cytol Histol 1989;11:219-24.
28. Böcking A, Auffermann W, Vogel H, Schlöndorff, Goebbels F. Diagnosis and grading of malignancy in squamous epithelial lesions of the larynx with DNA cytophotometry. Cancer 1985; 56:1600-4.
29. Gschwendtner A, Kreczy A. DNA cytometry: diploid standard and section thickness. Am J Clin Pathol 1994;102:558-9.
30. Gschwendtner A, Mairinger T. How thick is your section? The influence of section thickness on DNA-cytometry on histological sections. Anal Cell Pathol 1995;9:29-37.
31. Xin X, Sudbi J, Boysen M, Reith A. Caveats in the use of paraffin sections for DNA assessment in nuclei as demonstrated by confocal laser scanning microscopy. Anal Quant Cytol Histol 1996; 18:104.
32. Neter J, Kutner M, Nachtsheim C, Wasserman W. Applied linear statistical models. 4th ed. Chicago: Irwin; 1996.
33. Larsen LE, Walter DO, McNew JJ, Adey WR. On the problem of bias in error rate estimation for discriminant analysis. Pattern Recognition 1971;3:217-23.
34. Raudys SJ, Jain AK. Small sample size effects in statistical pattern recognition: recommendations for practitioners. IEEE Trans Pattern Analysis Machine Intell 1991;3:252-64.
35. Schulerud H, Kristensen G, Liestøl K, Vlatkovic L, Reith A, Albregtsen F, et al. A review of caveats in statistical nuclear image analysis. Anal Cell Pathol 1998;16:63-82.
36. SAS Institute Inc. SAS/STAT software: changes and enhancements through release 6.12. Cary (NC): SAS Institute; 1997.
37. Verbeke G, Molenberghs G, editors. Linear mixed models in practice, a SAS oriented approach. New York: Springer-Verlag; 1997.
38. Searle S. Linear models for unbalanced data. New York: John Wiley; 1987.
39. Hochberg Y, Benjamini Y. More powerful procedures for multiple significance testing? Stat Med 1990;9:811-8.
40. Scheffe H. The analysis of variance. New York: John Wiley; 1959.
41. MacAulay C, Palcic B. Fractal texture features based on optical density surface area: use in image analysis of cervical cells. Anal Quant Cytol Histol 1990;12:394-8.